FTD-ID(RS)T-0742-90

FOREIGN TECHNOLOGY DIVISION

SECOND-HARMONIC GENERATION OF TEA CO_2 10.6 MICROMETER LASER LIGHT IN $AgGaS_2$ CRYSTALS

by

Zhang Bangmin and Wang Dinghua

A-1

HUMAN TRANSLATION

FTD-ID(RS)T-0742-90 3 May 1991

MICROFICHE NR: FTD-91-C-000343

SECOND-HARMONIC GENERATION OF TEA CO_2 10.6 MICROMETER LASER LIGHT IN $AgGaS_2$ CRYSTALS

By: Zhang Bangmin and Wang Dinghua

English pages: 9

Source: Zhongguo Jiguang, Vol. 10, Nr. 6, 1983, pp. 339-342

Country of origin: China
Translated by: Leo Kanner Associates
F33657-88-D-2188
Requester: FTD/TTTD/Armstrong

GRAPHICS DISCLAIMER

All figures, graphics, tables, equations, etc. merged into this translation were extracted from the best quality copy available.

SECOND-HARMONIC GENERATION OF TEA CO_2 10.6MICROMETER LASER LIGHT IN $AgGaS_2$ CRYSTALS

Zhang Bangmin and Wang Dinghua, Anhui Institute of Optics and Fine Mechanics, Chinese Academy of Sciences

Abstract: Characteristics of $AgGaS_2$ crystal for frequency doubling of TEA CO_2 10.6micrometer laser light were investigated. When the crystal was 4.3mm long, the maximum conversion frequency was 0.122percent. The experimental phase matching angle was 71.5^{o} and the adjustment range was $8^{o}\pm1^{o}$. These data are in good agreement with the theoretical values.

I. Foreword

In recent years, much progress was made in expanding the range of laser wavebands by utilizing the nonlinear effects. In the medium-infrared waveband, the CO_2 laser is a relatively ideal light source and can output tens of laser spectral lines within the range 8.7 to 11.8micrometers. With double frequency, tunable output can be obtained within the range 4.3 to 5.9micrometers. Since the advent of CO_2 lasers, researchers have conducted numerous research tasks [1-3] in this area. However, since it is relatively difficult to obtain high-quality and large infrared nonlinear optical crystals, such work still remains at the laboratory research stage without practical applications. Chalcopyrite type three-element semiconductor compound crystals (such as $AgGaS_2$, $AgGaSe_2$, $CdGeAs_2$, and $CdGeP_2$, among others) are

outstanding materials that are viewed as promising in applications in this regard. The authors utilized two $AgGaS_2$ crystals grown in their laboratory in conducting double-frequency experiments on TEA CO_2 10.6micrometer lasers. Type I, double-frequency output with peak power of 2.7kW was obtained.

II. Selection of $AgGaS_2$ Crystals and Phase-Matching Mode

$AgGaS_2$ is a chalcopyrite type three-element semiconductor of the 42m point group; its light transmission waveband is 0.5 to 13micrometers; the nonlinear coefficient $d_{36}=(3.2\pm0.6)\times10^{-8}$esu. For $AgGaS_2$, its birefrigence is small and the variation of the refractive index is very weak. Therefore, in this experiment type I critical phase-matching mode was adopted (00-e). According to the working formula for calculating the effective nonlinear coefficient d_{eff}:

$$d_{eff}=d_{36}\sin\theta_m\sin2\varphi \qquad (1)$$

In the equation, d_{36} is the crystal nonlinear coefficient; θ_m is the phase-matching angle; φ is the azimuth angle. For d_{eff} at the maximum, $\varphi=45^o$ is selected. For type I phase-matching, the phase-matching angle $\theta_m=70.9^o\pm0.5^o$ of $AgGaS_2$ can be calculated according to nonlinear theory [4, 5].

Since the energy flow direction of the light beam was perpendicular to the curved surface of the reflector index, under the type I critical phase-matching situation, generally θ_m is not equal to 90^o; the angle of divergence ρ is formed by the direction of the energy flow of the anomalous light wave beam (secondary harmonic) and the equal-phase surface direction of propagation. For $AgGaS_2$, when $\theta_m=70.9^o$, $\rho=0.745^o=13$mrad.

The length l_a of the aperture effect is

$$l_a=a/\rho$$

The quantity a is the diameter of the light beam on the light passage surface of the crystal. When a=6mm, the length of the

aperture effect of $AgGaS_2$ was 461.5mm. When the crystal thickness was 5mm, and the wavelength of the fundamental wave was 10.6micrometers, the external allowable angle was $(\delta\theta)^{I}_{FWHM}$=72mrad.

Crystals used for experimentation were grown by using the crucible-lowering method and sliced according to type I phase-matching. The specimen was annealed and buffed with light-yellow, homogeneous, transparent and absence of macroscopic defects such as twinning, fissures, gas bubble inclusions, and other defects. Fig. 1 is a conical light diagram of similar specimens. Table 1 lists the main parameters of two specimens.

Fig. 1. Conical light diagram of $AgGaS_2$

III. Experimental Setup

Fig. 2 shows the optical path diagram of the experimental setup.

The CO_2 laser used in the experimentation was a semi-outer cavity type TEA CO_2 laser; its output light beam divergence was smaller than 10mrad and the diameter of the cross section of the largest light spot was φ=7mm at a distance of 30cm from the output length. The single-pulse output energy was 0.45J with pulse duration of 180ns and the peak value power density was 8.8MW/cm^2. As the output length was approached (R=∞ germanium level plate), a 4mm-thick ZnS plate was placed for polarization,

TABLE 1

编号 a	通光截面 (毫米) b	平均厚度 (毫米) c	楔形角* d	切割方式 e		对10.6微米的吸收系数 (厘米$^{-1}$) f
				θ	φ	
1	18×14	4.3	2.88'	67 5°	45°	0.25
2	10×8	5.2	35'35"	67.5°	5°	0.35

Remark: *The wedge-shaped angle was formed incidentally because of poor control during processing.
KEY: a - Number b - Cross section of light passage (mm) c - Average thickness (mm) d - Wedge-shaped angle e - Cutting method f - Absorption coefficient (cm^{-1}) for 10.6micrometers

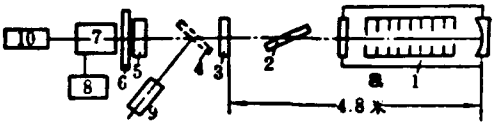

Fig. 2. Experimental setup
KEY: a - 4.8 m

becoming a Brewster angle insert with angle deviation $\pm 1^{o}$ to ensure that the output was linearly polarized light.

The reflector lens 4 served for adjusting the optical path. After the optical path was well adjusted, this reflector lens was moved out of the optical path. For the specimen adjustment frame, an optical theodolite adjustment was selected with an adjustment precision of 20s/graduated partition, capable of estimating an reading to within 6". When placing the two $AgGaS_2$ crystals, it had to be made certain that the plane formed by the crystal optical axis and the normal to the light passage surface was perpendicular to the polarized plane of the 10.6micrometer

laser beam. To facilitate adjustment, the polarized plane of 10.6micrometers in the experiment used the plumb direction. Filter 6 was a sapphire (Al_2O_3) crystal with a thickness of 1mm. Thus all of the 10.6micrometer could be filtered; for double-frequency light, the transmission index $T_{5.3}$=67percent. Items 9 and 10 are a He-Ne laser for tuning the optical path.

IV. Experimental Results

1. Relation between double-frequency efficiency and pumping power

In a situation of relatively low conversion efficiency, the conversion efficiency η for type I matching is determined by the following equation [1]:

$$\eta = P_{\omega_2}/P_{\omega_1}$$
$$= 2k^3\omega_1^2 d_{eff}^2 l^2 \frac{P_{\omega_1}}{A} \cdot \frac{\sin^2\left(\frac{\Delta Kl}{2}\right)}{\left(\frac{\Delta Kl}{2}\right)^2} \qquad (3)$$

In the equation, $P_{\omega 1}$ and $P_{\omega 2}$ are, respectively, the fundamental wave and double-frequency light power; k is the crystal plane wave impedance (k=377/refractive index), and ω_1 is the frequency of the fundamental wave; A is the light beam area of the fundamental wave and the secondary harmonic; ΔK is the wave vector mismatch; and l is crystal length.

Without focusing, the fundamental wave light beam can directly etch the crystal; the fundamental wave power was modified with an attenuator outside the cavity. At maximum power (8.8MW/cm^2), there was no damage to the crystal surface or inside the crystals. Fig. 3 is the relation curve of η versus $P_{\omega 2}$ obtained in the experiments. From the figure, within the power range used within the experiments, the results obtained agreed fairly well with the calculated results from Eq. (3); without the saturation phenomenon, the double-frequency

efficiency can be possibly further improved. However, limited by the power level of the CO_2 laser device, no further experiments were conducted. In actual measurements, the highest output power at 5.3 micrometers was 2.7kW and the highest conversion efficiency

η=0.122percent.

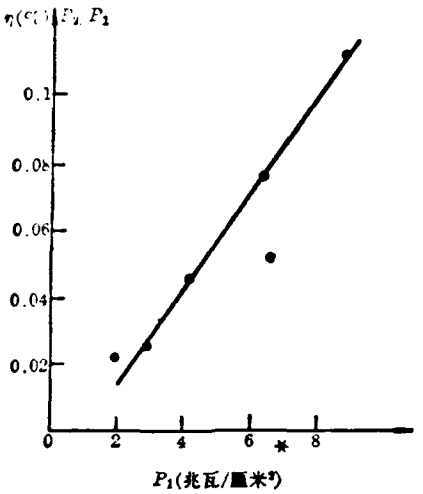

Fig. 3. Relation curve of η versus $P\omega_1$ of No. 1 $AgGaS_2$
KEY: * - P_1 (MW/cm^2)

2. Relationship between phase-matching angle and double-frequency light power

Since the birefringence of $AgGaS_2$ is low, the tuning range of angle is relatively wide, theoretically estimated at $8.8^o \pm 1^o$. Figs. 4 and 5 are, respectively, the measured angle-tuning curves of specimens 1 and 2; the total width of adjustment was $8^o \pm 1^o$, close to the theoretically estimated value, and also consistent with the data of [1, 2]. The optimal matching angle of 71.5^o was very close to the calculated value of 70.9^o.

When the crystal optical axis was in a horizontal plane, the polarized plane of 10.6micrometers was the plumb direction; then

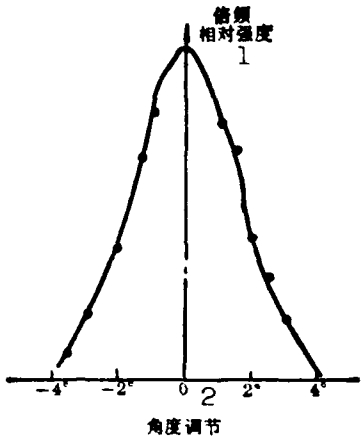

Fig. 4. Angle-tuning curve of No. 1 $AgGaS_2$ specimen
KEY: 1 - Relative intensity of double frequency
2 - Angle adjustment

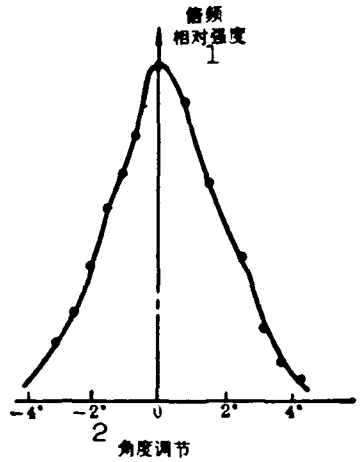

Fig. 5. Angle-turning curve of No. 2 $AgGaS_2$ specimen
KEY: 1 - Relative intensity of double frequency
2 - Angle adjustment

adjust the matching angle to the optimal position (θ_m), and estimate the dip and elevation angle to adjust the influence of $\Delta\varphi$ on the double-frequency output. The adjustment in this direction actually serves to change the azimuth angle φ and will influence θ.

(1) The variation ratio K can be expressed as:

$$K = \frac{\sin 2(\varphi + \Delta\varphi) - \sin 2\varphi}{\sin 2\varphi}$$
$$= 2\cos(2\varphi + \Delta\varphi)\sin\Delta\varphi$$

Substitute the initial angle φ=45° in the above equation:

$$K = 2\sin^2(\Delta\varphi)$$

Table 2 lists the calculated values of $\Delta\varphi$ versus K.

(2) The effect on matching angle θ due to $\Delta\varphi$

As shown in Fig. 6, the relationship between $\Delta\varphi$ and θ can be obtained by utilizing a simple geometric relationship:

TABLE 2

$\Delta\varphi$	2°	4°	6°	8°	10°
K	0.002	0.009	0.01	0.038	0.06

$$\cos\theta = \frac{1+\cos^2\theta_m-\sin^2\theta_m-4\cos^2\theta_m\sin^2\left(\frac{\Delta\varphi}{2}\right)}{2\cos\theta_m}$$

In the equation, θ_m is the optimal matching angle when the optical axis is in the horizontal position; for the specimens used in the experiment, $\theta_m=71.5^o$. Table 3 lists the calculated data for $\Delta\varphi$-$\Delta\theta$ ($=\theta_m-\theta$).

TABLE 3

$\Delta\varphi$	4°	6°	8°	1·°
$\Delta\theta$	0.05°	0.11°	0.20°	0.3°

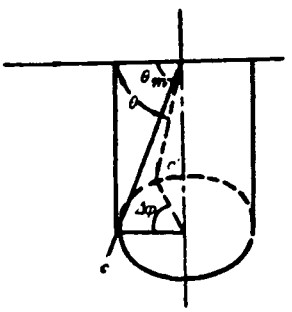

Fig. 6

From the above-mentioned calculated results, the effect on double-frequency can be neglected (wider tuning angle for $AgGaS_2$) when $\Delta\varphi$ is relatively small; the experimental results are basically in agreement with the estimated results. Of course, for crystals with narrow tuning width for certain angles, the effect of $\Delta\varphi$ cannot be neglected.

The $AgGaS_2$ crystals used in the experiments were provided by the growth section; comrade Xu Baojian assisted in processing the

crystals, and comrade Liu Laibao was of much assistance in orienting the crystals. The authors are grateful to the above-mentioned section and persons.

Zhao Meirong, Yin Hong, Yang Lin, and Wang Chao participated in the research. The paper was received on 23 September 1982.

REFERENCES

[1] Kupecek, J. and A. Schwartz, IEEE J. Quant. Electgr. QE-10/7, 540 (1974).

[2] Body, G. D., iEEE J. Quant. Electr. QE-7/12, 563 (1971).

[3] Jiateng Lie and Yingtien Zhishi [two Japanese names are transliterated according to the pronunciation of the Chinese characters], 50/7, 763 (1981).

[4] Kogan, R. M. et al., Advances in Laser Engineering 22, 71, California.

[5] Shen, Y-R., ed., Nonlinear Infrared Generation Topics in Applied Physics, Vol. 16, 1977.

DISTRIBUTION LIST

DISTRIBUTION DIRECT TO RECIPIENT

ORGANIZATION	MICROFICHE
C509 BALLISTIC RES LAB	1
C510 R&T LABS/AVEADCOM	1
C513 ARRADCOM	1
C535 AVRADCOM/TSARCOM	1
C539 TRASANA	1
Q591 FSTC	4
Q619 MSIC REDSTONE	1
Q008 NTIC	1
E053 HQ USAF/INET	1
E404 AEDC/DOF	1
E408 AFWL	1
E410 AD/IND	1
F429 SD/IND	1
P005 DOE/ISA/DDI	1
P050 CIA/OCR/ADD/SD	2
AFIT/LDE	1
NOIC/OIC-9	1
CCV	1
MIA/PHS	1
LLYL/CODE L-309	1
[redacted]	1
NSA/T513/TDL	2
ASD/FTD/TTIA	1
FSL	1